NUMERICAL DESIGN AND OPTIMIZATION OF A NEW CASING TREATMENT FOR SHROUDED FANS

L. Soulat[1⋆], S. Moreau[2], P. Ferrand[1], S. Aubert[3], M. Henner[4]
[1]Laboratoire de Mécanique des Fluides et d'Acoustique, Université de Lyon, Ecole Centrale de Lyon; Université Lyon 1; INSA Lyon; CNRS UMR 5509, France
[⋆](Currently at GAUS - laurent.soulat@usherbrooke.ca)
[2]GAUS, Département de Génie Mécanique, Université de Sherbrooke, Canada
[3]Fluorem SAS, France
[4]Valeo Engine Cooling, France

Keywords: *casing treatment, helicoidal grooving, shrouded fan*

Abstract

The gap flow is responsible of high losses of efficiency for shrouded fan. This paper presents a new casing treatment consisting in a helicoidal grooving of the hub which is designed to reduce the massflow and the swirl of the gap flow. This device is studied through numerical simulations. It is first described, validated and analyzed using a simple canonical geometric model. The resulting complex flowfield is precisely analyzed, and the casing treatment is then characterized and optimized. An optimized geometry is applied to a test fan, achieving both leakage and swirl reduction.

1 Introduction

For modern turbomachines, the necessary clearance between casing and rotors is a major problem regarding efficient design. It is well known that this clearance is responsible for some secondary flows impinging the "main" flow, thus generating aerodynamic losses and/or flow patterns that can trigger some instabilities (e.g. surge). For axial compressors such as fans, the clearance is usually responsible for the biggest part of the efficiency drop. These effects may vary, depending on the size of the gap and the geometry of the machine.

For the particular case of shrouded fans studied here (Fig. 1), blades are linked together by a tip ring. This system is generally used to ensure stronger mechanical properties of the row and improve the fan acoustic (reduce fan noise). For this configuration, two problems arise from the gap flow.

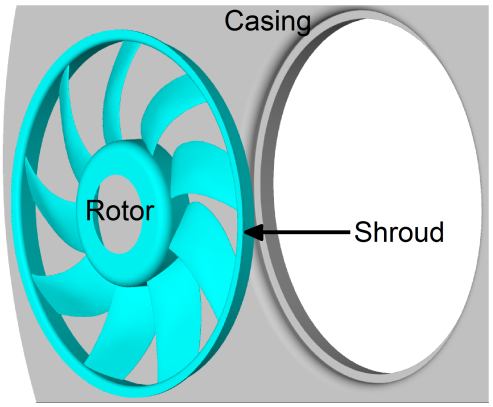

Fig. 1 Exploded view of a shrouded fan

At first, the tip clearance flow does not impinge directly the main flow around the blade : it develops through a cylindrical channel limited, on one side, by the outermost surface of the rotating ring, and on the other side, by the inner surface of the casing. The interaction with the main flows occurs only upstream and downstream of the row. Since this flow is mainly driven by the mean axial pressure gradient through the blade

row, fluid exits the gap and interacts with the main flow only upstream of the compressor row. Because of the pressure rise through the rotor, fluid circulate within the gap from the outlet toward the inlet of the compressor, thus reducing the overall 'useful' massflow of the rotor and the achievable compression rate. For a fan, which is designed to insure a high massflow at a certain pressure rise (to overcome the viscous loss in the system), this is clearly a problem. The second characteristic is related to the geometry of the gap. The gap flow is subject to a high circumferential shear between rotor and casing. As a consequence, the flow quickly accelerate in that direction, acquiring an important tangential mean velocity. This effect is even worse when the fluid enters the gap with swirl. This velocity is then communicated to the main flow due to viscous mixing when gap flow exits, generating (for compressors) an unwanted pre-swirl in the tip region. The resulting off-design inlet flow conditions are responsible for increased aerodynamic losses.

To limit the gap flow effects, the simple solution is perhaps to use a casing treatment. One can find several systems in literature, such as labyrinth seal [9, 10], vortex seal, or even 'bladelets' [8], but none of these systems is designed to reduce on both leaking massflow and swirl. For instance, labyrinth can increase the swirl if the fin are mounted on the rotor (bigger moving surface). Moreover, they are generally designed to operate efficiently in particular conditions, such as small gap [6]. Therefore, a new type of casing treatment will be proposed in this article. It consists of an helicoidal grooving of the casing, aiming at reducing both the leakage massflow and the exit swirl. The bent grooves are intended to provide some fluid guidance in order to *limit the outlet swirl*, but also to provide some blockage so as to *limit the massflow and increase the mean axial pressure gradient through the gap*. From this point of view, the higher the aerodynamic losses, the better. In the presently studied low-speed cooling fan (Fig. 1), this device is interesting because it has an important gap (due to assembly constraint, the clearance g is about a few millimeters, leading to a ratio g/h_b of 2% where h_b is the blade height). This unusual point is interesting to prove the robustness of the new casing treatment. The casing treatment is numerically studied here. Its geometry and the numerical parameters are described in the next two sections. The flow field structure is analysed next. Finally, the parameterization with several geometric parameters is achieved to yield an optimal configuration.

2 Description of the new casing treatment

To comply with the first part of the study, i.e. validating the concept and analyzing the flowfield generated by the grooves, the casing treatment and the gap are first modelled in a simple way. At this point, it is not relevant to introduce specific technological effects to keep the most general approach as possible. This implies to use a flat geometry with sharp angles (Fig. 2). The rotor is simulated by a plan with a uniform translation movement. It slides above the casing wall and the grooves. Only one groove is simulated since periodicity in the transversal direction can be assumed. The rotor blades are not simulated at this point to simplify and to keep the case as general as possible. Nevertheless, the fluid is supposed to enter the gap with some swirl, imposed to mimic (grossly) what can be seen with a full simulated rotor.

The geometry is described using five parameters (Fig. 2) :

- α is the helix angle. By convention, α=90° accounts for axial grooves, α>90° (resp. <) stands for grooves grossly opposed (resp. aligned) to the swirling incoming fluid.
- h is the groove's height. Please note that the "rotor" is located 2mm above the grooves, whatever the value of h is. This means that the total gap height is h+2mm.
- w is the groove's width.
- L is the groove length. For the tested geometry, it was chosen not to extend the grooves over the wall casing to keep a degree of freedom. Hereafter, the casing is

about 27mm long, the grooves start at 9mm from the gap entrance.

- N is the number of grooves. For a flat model, this parameter essentially accounts for the total width of the simulated channel, and, since the groove's width w is set, for the width of the wall separating the grooves. It thus requires a "radius" R_0, chosen to be 155mm from the selected fan geometry.

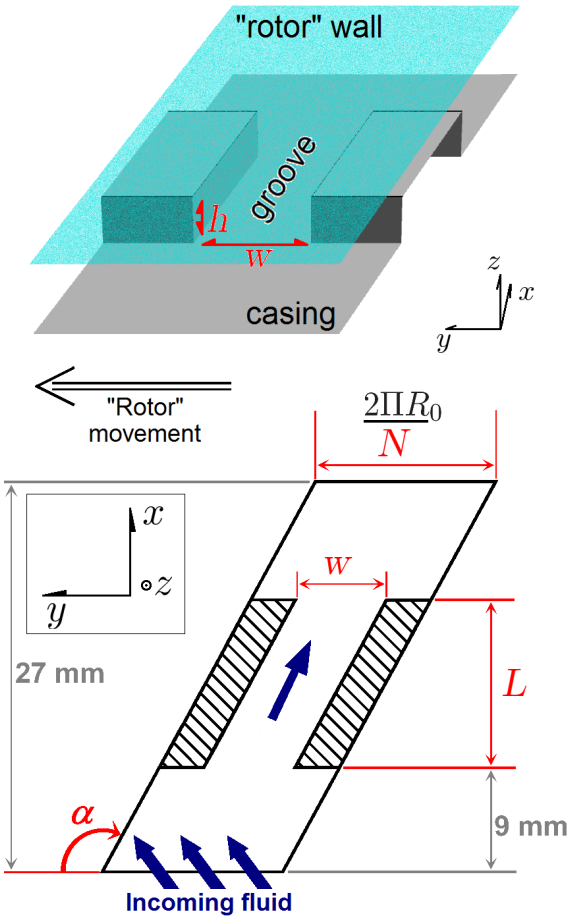

Fig. 2 Groove modelization

3 Numerical simulation and criteria

This study is based on two numerical approaches. On the one hand, the validation and the flow description around the treatment is done using the RANS commercial solver Turb'Flow^{TM} [2]. In this case, time integration is done with a five steps Runge-Kutta time marching algorithm. The spatial discretization is based on a MUSCL finite volume formulation with vertex variable storage. The Liou's Advection Upwind Splitting Method [4] is used to calculate the convective fluxes, and the viscous terms are determined through a second order spatial scheme. The turbulence model is the Kok's k-ω [3]. On the other hand, the special high-order parametric flow solver Turb'Opty^{TM} is used to achieve the parametric study of the casing treatment [5]. This method relies on a derivation of the discretized Navier-Stokes equations. High order derivatives of the flowfield can therefore be calculated from a reference configuration. Other configurations are then extrapolated using an adequate formulation. In this study, first- and second-order derivatives of the conservative variables have been calculated for each parameter, and the extrapolation is achieved with Fourier's series. The main advantage of this technique is that the time for extrapolating any solution is negligible, and the calculation of all the derivatives is equivalent or less than a single RANS calculation. As a result, it is materially possible to evaluate thousands of configuration with the parametric technique, whereas the direct RANS approach is far too much time-consuming (several years).

In both cases, the numerical simulations assume that inlet massflow and outlet static pressure are imposed. In these conditions, it is not possible to see any massflow reduction due to the casing treatment. Therefore, the next sections focus on the blockage criteria for the groove, which can be measured using the mean static pressure difference ΔP_s between the inlet and outlet of the gap. This criterion is usually negative and should be maximized in absolute value. The swirl variation within the gap is measured with the mean transversal velocity difference ΔV_y. Since inlet swirl is imposed, this criterion directly accounts for the exit swirl. It has to be minimized. A third criterion is used to quantify the energy exchange within the groove : it is the mean total pressure difference ΔP_t that can shows whether the fluid

gain or lose energy while passing through the gap. This criterion should be as negative as possible.

4 Concept validation

Before analyzing the flowfield, it is relevant to validate the concept of this casing treatment. In the following, the configuration used is [α=115°, h=3mm, w=7.8mm, L=9mm, N=50]. This configuration is compared (on the three criteria ΔP_s, ΔV_y and ΔP_t) to a simple straight gap with the same height (i.e. h+2mm clearance), that illustrates the case without any treatment, and to a gap fitted with a simple fin, i.e. the case of a simple labyrinth seal. The latter was simulated using 0-width grooves with L=9mm and h=3mm. Results are listed in the table 1.

Config.	ΔP_s [Pa]	ΔV_y [m/s]	ΔP_t [Pa]
Simple gap	-7.5	5.25	60.9
Single fin	-54.6	6.04	34.1
Grooves	-31.6	2.89	1.7

Table 1 Casing treatments performances

As one can see, the new casing treatment clearly improves the blockage and the outlet swirl compared to the simple gap. Even if it cannot create as much blockage as the single fin (which shows the lowest section of the three cases), the new treatment improves dramatically the swirl and the energy exchange. The helicoidal grooving is therefore valid since it improves the gap flow, and provides a good compromise between the simple gap and the single fin with respect to the three criteria.

5 Flowfield analysis of the reference configuration

In the present study, the reference configuration is [α=115°, h=3mm, w=7.8mm, L=9mm, N=50]. The velocity field in two "blade-to-blade" planes, (Fig. 3) at mid-height of the groove and mid-height above the groove shows that the groove effectively guides the fluid in the lower section of the gap. In the upper section of the gap (i.e. between the groove and the rotor wall), the flow is almost uniform, with a strong transversal movement caused by the rotor. As previously stated, the transversal velocity increases while passing through the gap. Because of the viscous mixing, this transversal movement reappears at the bottom of the gap downstream of the groove.

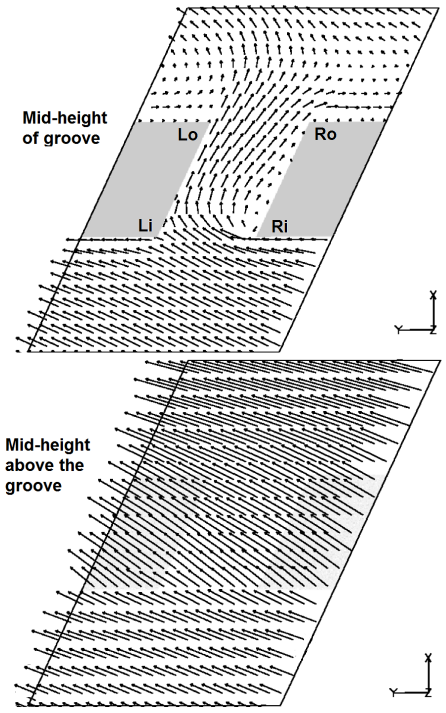

Fig. 3 Global velocity field

Even if the overall flowfield structure is simple, a detailed analysis reveals up to five distinct vortices interacting together. For a sake of clarity, the entrance left and right corner of the groove are called Li and Ri, as well as the exit corners Lo and Ro (Fig. 3).

5.1 Entrance vortex

The first vortex, or "entrance vortex", is located near the corner Ri. It is merely a detachment of the fluid caused by the high turning angle at this location (Fig. 4).

This structure is important for the massflow reduction since it generates a backflow near the wall and thus a reduction of the passing section of the gap. It is also highly dissipative.

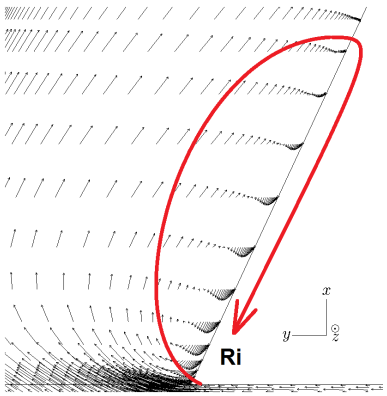

Fig. 4 Entrance Vortex

This vortex is clearly linked to the groove angle α, but the relationship is non linear. The furthest position of the reattachment point is achieved for α around 110°. Indeed for lower angles, the vortex is naturally small because of the low deviation of the incoming fluid ; for higher angles, the vortex decrease because of the massflow reduction within the groove (high angles are responsible for a high blockage of the groove). This structure is also slightly sensitive to the groove width : a large groove will lead to a large vortex.

5.2 Groove vortex

The second vortex, or "groove vortex", is located within the groove, but unlike the first one, it develops along the groove axis (Fig. 5)

This vortex is interesting for the swirl criterion since it tends to generate a transversal velocity opposed to the main swirl at the bottom of the groove. This velocity comes in addition to the groove natural guidance. This vortex can be seen as a passage vortex since the walls Li-Lo and Ri-Ro stand respectively for a pressure side and a suction side of a (poorly-shaped) blade. It is also similar to a scraping vortex as the fluid circulating above the groove dives when encountering the wall Li-Lo.

As it can be seen with streamlines in Fig. 5, this vortex interacts directly with the entrance vortex : fluid particles involved in the first one are latter convected and form the heart of the groove vortex.

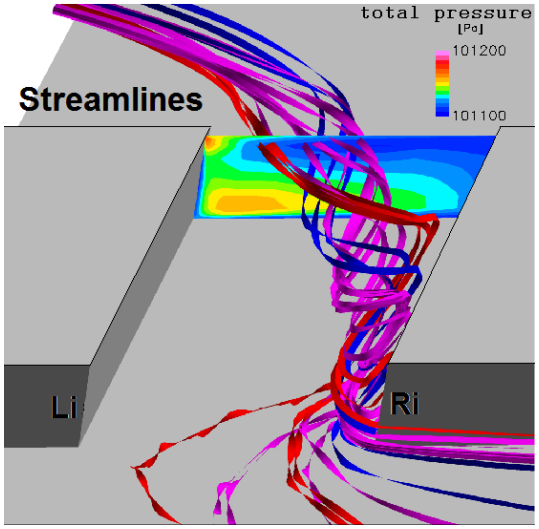

Fig. 5 Groove vortex

This vortex is mainly sensitive to the angle α, the height h and the width w, parameters that modify its trajectory and intensity : a shallow and/or large groove will intensify its structure.

5.3 Rear vortices

The last three vortices lie in the wake of the wall separating the grooves. They are essentially detachments. The first is visible in a meridional plane (Fig. 6). It is basically like the well documented backward facing step vortex, even if it does not share the characteristics of the latter: it is shorter because the wall is not infinite in the transversal direction here.

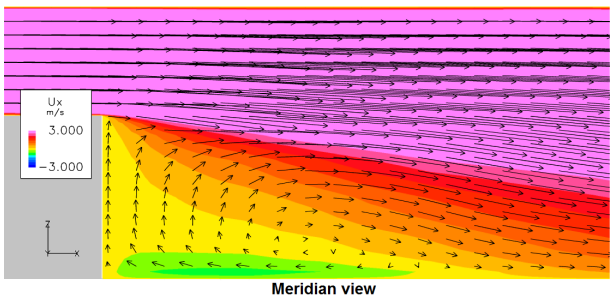

Fig. 6 Meridian rear vortex

The main effect of this meridional structure is the generation of a backward flow near the casing. It is sensible mainly to the groove height h and the w and N parameters that modify the

wall's width. The bigger the wall is, the larger the vortex will be.

The other two vortices develop in the blade-to-blade plane. Both are flow separations occurring past the Ro and Lo corners. These two structures are represented in Fig. 7 for a helix angle α=45°.

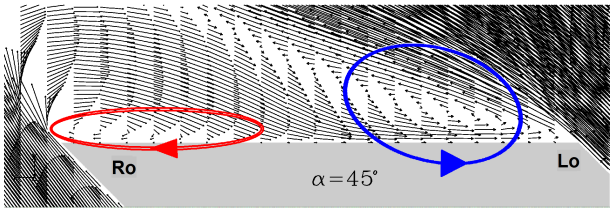

Fig. 7 Blade-to-blade rear vortices

The vortices are counter-rotating, with a close interaction since they are separated only by the wall's width. The interaction is useful for the swirl reduction because a massive transversal flow opposed to the rotor movement can be observed. The viscous dissipation is also interesting for the blockage criterion.

These structures are highly sensitive to the helix angle α. For instance, the Ro-detachment grows when α decrease, and the Lo-detachment grows along with α. Parameters h, w and N also affect these structures by modifying the size of the wall and its wake.

The last noticeable point for the rear vortices is the complete interaction between the meridional and the blade-to-blade structures. The coupling generates a complex structure that can extend in front of the groove exit. For high helix angle, it was noted that the resulting structure generates a backflow (negative axial velocity) near the casing across the groove end section, thus potentially limiting the massflow through the gap.

5.4 Possible technological effects

It is necessary to validate the basic assumption of the model (sharp angle, flat geometry) since the associated technological effects can greatly modify the flowfield. A flat geometry with 0.3mm radius fillet was simulated. All the described vortex are present, some being slightly altered. Another cylindrical geometry with sharp edges was also tested, with no significant difference with the plane configuration (Fig. 2). In both cases, the aerodynamic criteria are nearly the same than in the present simplified model.

6 Parametric study

The study of the sensitivity of the criteria to various parameters underlines some interesting trends for the application of the casing treatment. The parameterization is achieved with the unique parametric Navier-Stokes solver Turb'OpTy^{TM}. The five parameters described in section 2 are first studied separately. Their coupling is then considered and the final optimization is presented.

6.1 Groove length L

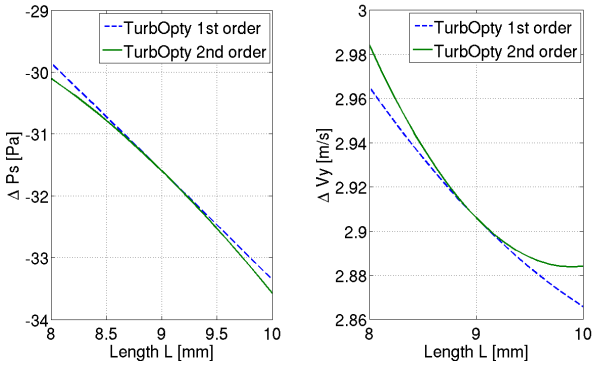

Fig. 8 Effects of the parameter L

The variation of the criteria with respect to the parameter L are shown in Fig. 8. The first order (only the first order derivative is taken into account) and second order (first and second derivatives are used) variations are represented. As one can see, the length has a monotonic influence on the static pressure and swirl criteria. The total pressure criterion variation (not shown here) is also monotonic, so that we can conclude that long grooves are better for all criteria. It may also be noticed that the static pressure variation is essentially linear. Second order effects are only visible for the swirl criterion.

6.2 Groove width w

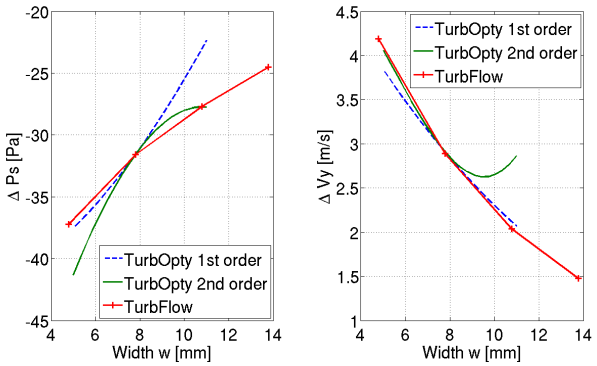

Fig. 9 Effects of the parameter w

Fig. 9 represents the variation of the static pressure and swirl criteria with respect to the groove width w. The total pressure criterion evolution is similar to the swirl. Some direct calculations with the RANS solver Turb'Flow^{TM} are also represented for a validation sake. The most noticeable point is that for this parameter, static pressure and swirl/total pressure cannot be improved simultaneously. The first one demands narrow grooves (which is coherent with what was observed on the single fin during the validation), whereas the swirl reduction is better with large grooves (allowing a strong flow inside them).

This time second order effects are quite important for all criteria. The difference between the extrapolated variation and the direct simulation suggests that higher order effects can also be present. Therefore, it would be relevant to (at least) calculate third order derivatives.

6.3 Number of grooves N

The effects of the parameter N on the criteria are represented in Fig. 10.

Once again, the static pressure criterion is opposed to the other. Dealing with swirl or total pressure, the trends indicate that numerous groove are the best. Since the parameter N controls the wall width, grooves separated by thin walls are the most efficient for turning the flow within the gap. This is somehow similar to what has been seen for the parameter w. For a fixed

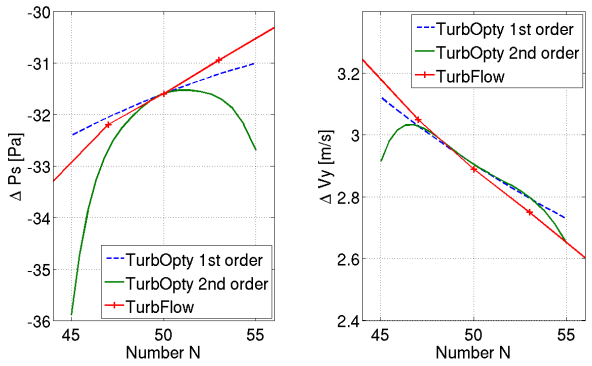

Fig. 10 Effects of the parameter N

number N, increasing w will lead to thin walls.

As can be noticed from the direct simulations, the variations are mainly based on some first-order physics, except for the static pressure. Yet, away from the reference (N=50±3), the second order extrapolation differs greatly from these direct simulations, which suggests that the truncation error of the reconstruction is not negligible any more. For this reason, the study will now be restricted to the interval [N=48,N=52].

6.4 Groove height h

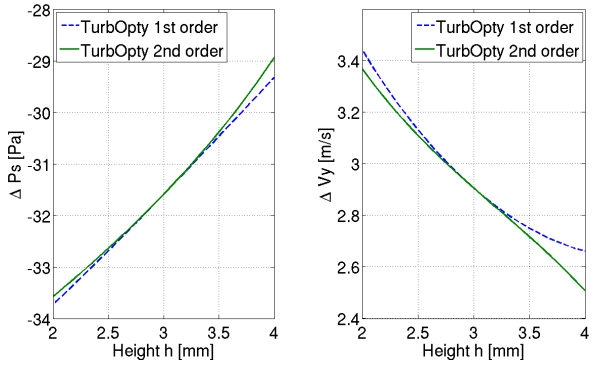

Fig. 11 Effects of the parameter h

The study of the influence of parameter h (Fig. 11) clearly indicates that shallow grooves are efficient for massflow reduction, but not for swirl reduction (once more, the total pressure objective behaves like swirl). This last point is quite obvious since it means that the gap is narrow and thus the transversal shear is at a high level. The static pressure drop may be more surprising.

Actually, this is coherent with the parameterization: it was chosen to keep the massflow constant independently from h, as well as the fluid incidence. This implies to reduce the mean axial velocity when increasing the height. In these conditions, it can be shown that for the same deviation of the fluid, the pressure gradients within and around the groove are stronger for low values of h. Aerodynamic losses are also increased for small height.

6.5 Helix angle α

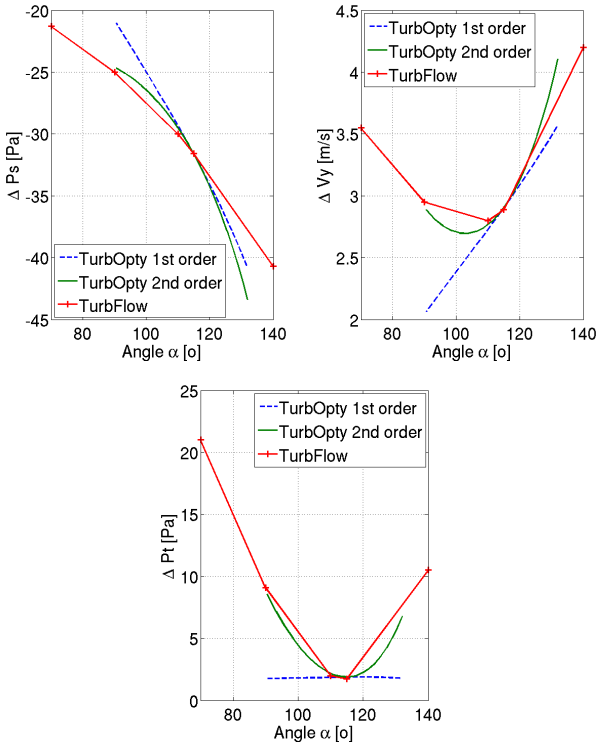

Fig. 12 Effects of the parameter α

This parameter exhibits very interesting trends. As shown in Fig. 12, the static pressure varies monotonically, decreasing toward high angle. The casing treatment asympotically therefore mimics the single fin for α tending to 180°.

The variations of ΔV_y and ΔP_t reveal that there is an optimum located approximately at $\alpha = 110°$. This result is confirmed by the good agreement between the extrapolated curves and the one obtained with direct simulation. This optimum can be explained as follows: for low angle, the measured massflow within the groove is high, but the fluid deviation is low, so that it does not counter the main swirl efficiently. On the contrary, at high angle, the deviation is very important, but because of the blockage within the groove, the massflow circulating through it is low, which results in a low swirl reduction capacity. At the optimum, a compromise is achieved between high massflow within the groove and high deviation of the fluid. In that case, the total pressure variation mainly accounts for the dynamic pressure variation.

6.6 Parameter coupling

The coupling between parameters is studied through the use of second order cross derivatives of the flowfield. For this casing treatment, couplings are generally low, except for h and L or w and L. In the first case, the coupling underlines that long and deep grooves are useful to improve ΔV_y, and for the second case, thin and long grooves are even more efficient to increase ΔP_s.

6.7 Casing treatment optimization

In order to be applied efficiently to the fan test case, the modelled casing treatment is optimized. This ***multi-objective multi-parameter*** optimization is achieved with the NSGA-2 genetic algorithm [1], coupled with the parameterization previously studied. Optimal population is reached in approximately 50 generations, for a total number of 100 generations of 500 individuals each. The Pareto-optimal population is analyzed thanks to a Self Organizing Map (SOM) algorithm [7]. In this type of representation (Fig. 13), each map represents one information (value of parameter or objective) over the population with the same topology, so that one point -one configuration- can be quickly found on every map.

The first thing to note is that some parameters are blocked at the limit imposed for the optimization. For instance, every optimum has a length L=10mm, which suggests that the optimization can be continued beyond this point. In the same approach, the number N takes only two values, N=48 and N=52.

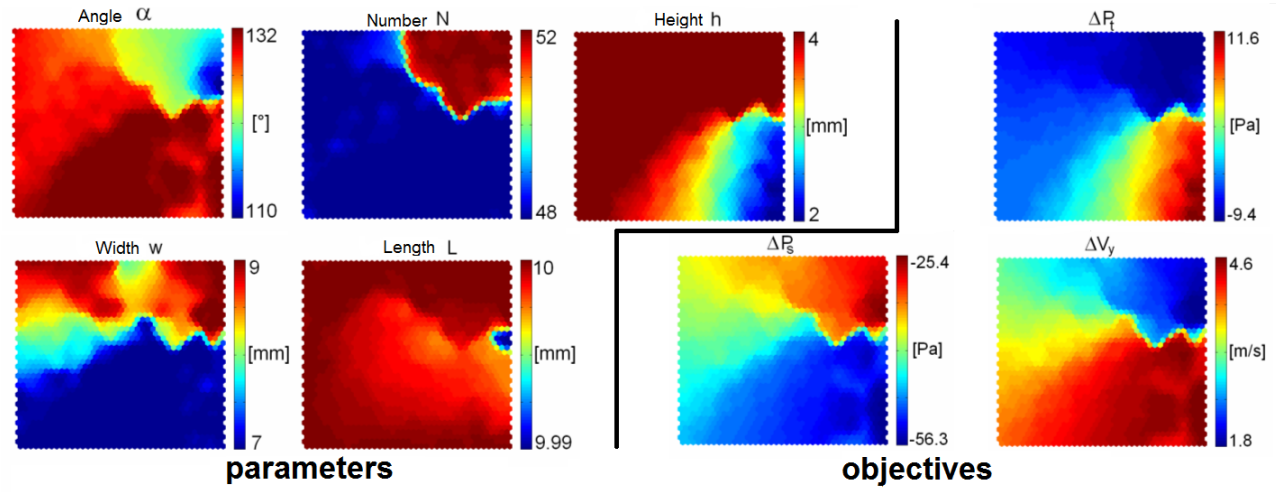

Fig. 13 SOM analysis of the optimal population

Other parameters vary in a smoother way. The clear opposition between ΔP_s and ΔP_t-ΔV_y is present in the optimal population. One can also find that the best individuals for ΔP_t and ΔV_y are slightly different, but both belong to a zone with low angle (around 115°), large height (4mm) and width (around 9mm). This is consistent with what as been previously noticed.

7 Application of the casing treatment on a test fan

A casing treatment geometry taken from the optimization is applied to the complete test fan. The chosen geometry is the one corresponding to the total pressure optimum. This geometry had to be slightly modified to satisfy the simulation condition (most notably the chorochronicity hypothesis), so that the applied geometry is [α=112°, h=3mm, w=8.5mm, L=10mm, N=54]. Yet, it was found that this casing treatment does not improve the flow within the gap relatively to the case with the standard gap. The reason of this bad performance is linked to the gap geometry of the studied fan.

As illustrated in the meridional cut of the gap for the test fan (Fig. 14), the rotor shroud is fitted with a labyrinth seal, i.e. a radial extension that creates elbows in the gap. Because of this device, the outlet vortex of the grooves is so much amplified that it totally closes the exit of the grooves, annihilating the massflow within them and making them ineffective.

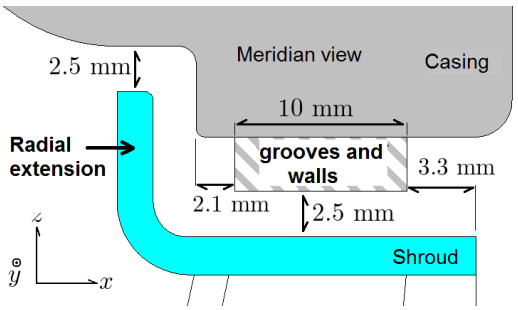

Fig. 14 Gap configuration for the test fan

To suppress this problem, longer grooves and smaller vortex seal are used (Fig. 15).

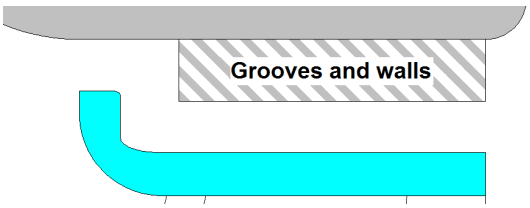

Fig. 15 Corrected gap configuration

With such a configuration, the gap flow is greatly improved.

As it can be seen in table 2, the massflow within the gap is almost divided by two with the casing treatment, the swirl rise is divided by almost 5, and the static pressure difference is multiplied by more than 2. From this point of view,

Config.	ΔP_s $[Pa]$	$massflow$ $[10^{-2}.kg/s]$	ΔV_y $[m/s]$
Standard gap	-97.5	2.58	5.02
Casing treat.	-208.7	1.42	1.04

Table 2 Gap flow characteristics

we can conclude that the new casing treatment is effective, reducing dramatically both swirl and leakage.

8 Conclusion

The casing treatment proposed in this paper has been validated from a simple canonical model to a real test case. This is an helicoidal grooving of the casing that allows to reduce both leakage and swirl for the gap flow in shrouded fan configurations. The precise description of the flowfield associated with this grooving has revealed several interacting vortices, as well as their sensitivity to some geometrical parameters defining the groove. The casing treatment has been characterized relatively to these geometrical parameters, and then optimized.

At this point, only the casing treatment was optimized. It would be relevant in future studies to also modify the fan, since late results have shown that the improvement of the gap flow induce a critical modification of the inlet flow over the blade tip. Therefore, the blade should be re-adapted, before optimizing simultaneously the casing treatment and the fan.

Acknowledgement

This study is part of the programs CINEMAS[2] (Région Rhône-Alpes) and LIBRAERO (Agence Nationale de la Recherche). Calculations were performed at CINES.

Copyright Statement

References

[1] K. Deb, S. Agrawal, A. Pratap and T. Myarivan. A fast elitist non-dominated sorting genetic algorithm for multi-objective optimization : NSGA2 *KanGAL report No. 200001*, 2000

[2] J. Caro, P. Ferrand, S. Aubert and L. Kozuch. Inlet conditions effects on tip clearance vortex in transonic compressor. *Proceedings of 5th European Conference on Turbomachinery Fluid Dynamics and Thermodynamics, Prague*, 2003

[3] J.C. Kok. Resolving the dependence on free-stream values for the k-ω turbulence model *AIAA Journal*, 38(7), 2000

[4] M.S. Liou. A continuing search for a near-perfect numerical flux scheme, part 1: AUSM+. *NASA Technical Memorandum TM106524*, 1994

[5] S. Moreau, S. Aubert, M. N'Diaye, P. Ferrand. Parametric study of a fan blade cascade using a new parametric flow solver Turb'Opty. *Proceedings of 4th ASME/JSME Joint Fluid Engineering Conference, Honolulu, Hawaii*, 2003

[6] G. Vermes. A fluid mechanics approach to the labyrinth seal leakage problem. *ASME Journal of Engineering for Power*, 83, 1961

[7] J. Vesanto, J. Himberg, E. Alhomieni and J. Parhankangas. SOM toolbox for Matlab5 *Report A57, Helsinki University of Technology*, 2000

[8] A.M. Wallis, J.D. Denton and A.A.J Demargne. The control of shroud leakage flow to reduce aerodynamic losses in a low aspect ratio, shrouded axial flow turbine. *Journal of Turbomachinery*, 123, 2001

[9] S.M. Wellborn, I. Tolchinsky and T.H. Okiishi. Modeling shrouded stator cavity flows in axial-flow compressors. *Journal of Turbomachinery*, 122, 2000

[10] H. Zimmermann and K.H. Wolff. Air systems correlation, part 1: labyrinth seal. *Proceedings of ASME Turbo Expo 1998, Stockholm, Sweden, 98-GT-206*, 1998